Direct Photolysis of Fenpyroximate in a Buffered Aqueous Solution under a Xenon Lamp

Mark B. Swanson,* William A. Ivancic, Adesh M. Saxena, Jeffrey D. Allton, and G. Kelly O'Brien

Battelle, 505 King Avenue, Columbus, Ohio 43201

Takashi Suzuki, Hideo Nishizawa, and Masaru Nokata

Nihon Nohyaku Company, Tokyo, Japan

Exposed to light from a xenon lamp of spectral intensity and wavelength distribution comparable to that of sunlight, fenpyroximate (**I**), a miticide manufactured by Nihon Nohyaku (Tokyo), degrades in neutral aqueous solution with a half-life of 1.5 h to form primarily its cis geometric isomer (**II**). The degradation of **II** was also measured and yielded a half-life of 10.5 h. The quantum yield of the phototransformation, 7.5%, was calculated directly from the absorption spectrum of **I**, the wavelength distribution of the light source, and the rate at which degradation occurred. This approach was selected rather than actinometry because it measures all parameters directly, does not depend on the additional assumptions inherent in actinometry, and requires only the parameters already requested in U.S. Environmental Protection Agency (EPA) guidelines. The rapid degradation of fenpyroximate and of its geometric isomer indicates that, when exposed to sunlight, they would not accumulate in an aqueous environment.

Keywords: *Photolysis; quantum yield; fenpyroximate; xenon lamp*

INTRODUCTION

Fenpyroximate (**I**), [*tert*-butyl (*E*)-α-[[[(1,3-dimethyl-5-phenoxypyrazol-4-yl)methylene]amino]oxy]-*p*-toluate] (Figure 1), a miticide manufactured by Nihon Nohyaku (Tokyo), was evaluated for its ability to photodegrade in aqueous buffer at pH 7 under a xenon lamp.

Traditionally, photolysis studies carried out to evaluate environmental impact have been performed under natural sunlight (Leifer, 1988). Since solar irradiance varies with annual and diurnal cycles and with weather, actinometers have traditionally been used. Actinometers, compounds whose interaction with light has been well-characterized, indicate the amount of energy with which a particular surface is actually irradiated by exposing them to the light source concurrently with the test compound (Leifer, 1988). Thoma and Kerker (1992) have documented the advantages and disadvantages of conducting photolysis studies using natural sunlight. One advantage is that the intensity and wavelength distribution will roughly match those actually encountered in the use of the product being tested. However, to fully characterize the wavelength distribution of natural sunlight would usually not be feasible, as it varies continuously with atmospheric conditions and with solar declination. This limitation constitutes a disadvantage in a photolysis study, since different wavelengths may generate different quantum yields (de Mayo and Shizuka, 1973; Dauben and Kellogg, 1971; Sugihara et al., 1985) or even different photodegradation products (Thoma and Klimek, 1985; Testa et al., 1979). This disadvantage may affect the outcome of a photolysis study because, although actinometry can accurately account for the irradiance of incident light, it does not necessarily account for the fluctuations in wavelength distribution typical of natural sunlight.

Thus, to provide for optimum reproducibility of results, it is necessary to characterize the wavelength distribution of a relatively stable source of light, in which case artificial light must be employed. According to the review by Thoma and Kerker (1992), artificial light sources are currently preferred for the quantitative testing of photostability. They also point out that, of the artificial light sources commercially available, the optically filtered xenon lamp provides a wavelength distribution (between 300 and 800 nm) more similar to that of sunlight than provided by other artificial sources, an important consideration when predicting a compound's environmental fate. Although this review dealt primarily with the pharmaceutical industry, the same principles can be expected to apply to agricultural chemicals.

As artificial light sources are used instead of natural sunlight for photostability testing, the practice of using chemical actinometers continues for purposes such as comparison between natural and artificial sources (Larson et al., 1991; Woodburn et al., 1993). Also, in the absence of spectral radiometric equipment, actinometers must still be used to calculate quantum yield, regardless of which light source is used.

Quantum yield is a parameter useful for predicting photodegradation of a compound under conditions (latitudes, seasons, and water depths) that may vary from experimental conditions (Zepp and Kline, 1977). Determination of quantum yield is recommended in guidelines for registration of relevant agricultural products by the German regulatory agency, Biologische Bundesanstalt (BBA) für Land- und Forstwirtschaft (1990). The U.S. Environmental Protection Agency (EPA) requires that photostability testing include (among other data) the absorption spectrum of the test compound, the wavelength distribution and intensity of the artificial light to which the sample is exposed, and the degradation rate of the test compound (U.S. Environmental Protection Agency, 1982). These three parameters suffice to calculate an average quantum yield directly, without recourse to actinometry. Therefore, it is un-

0021-8561/95/1443-0513$09.00/0

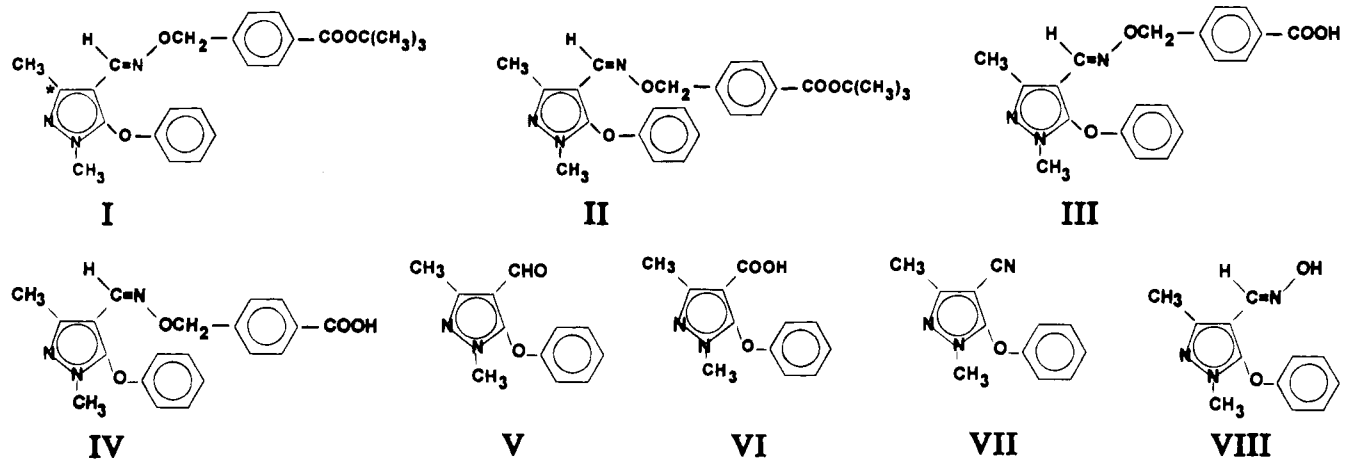

Figure 1. Structures of fenpyroximate and potential degradates. The asterisk (*) on the pyrazole ring of structure **I** indicates the position at which fenpyroximate was labeled with ^{14}C.

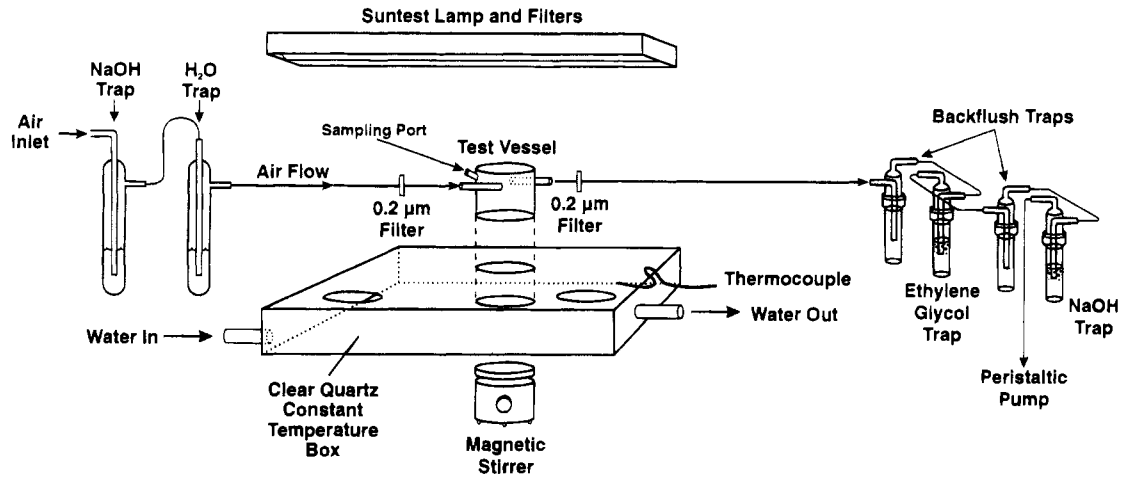

Figure 2. Apparatus shown containing one test vessel. Up to three test vessels were mounted simultaneously, each with its own system of traps.

necessary to routinely use actinometry in conjunction with a xenon lamp to meet the requirements of these regulatory agencies, since the xenon lamp generates a stable wavelength distribution (Bard, 1989). Thus, the requirements of both regulatory agencies (EPA and BBA) can be addressed simultaneously without including extraneous chemicals as actinometers. This paper sets out an example of how that can be accomplished.

Preliminary investigation (Nishizawa et al., 1990) showed that exposure of fenpyroximate to natural sunlight or xenon lamp initially yielded its geometric isomer (**II**) as the main product, which subsequently degraded upon prolonged irradiation. The purpose of the present study was to provide additional data to allow regulatory agencies to evaluate the fate of fenpyroximate in the environment. Due to the low aqueous solubility (14.7 ppb at 20 °C) and short photohalflife of fenpyroximate, the study was conducted in two phases:

Phase I was conducted on a time scale appropriate for calculating the first-order rate constant for the degradation of fenpyroximate (**I**), and phase II for that of the initial photolysis product (**II**) of fenpyroximate.

MATERIALS AND METHODS

Chemicals. [^{14}C]Fenpyroximate, labeled at carbon-3 in the pyrazole ring, specific activity 23 mCi/mmol (1.21×10^8 dpm/mg), radiopurity >98%, was supplied by Nihon Nohyaku Company, Ltd. (Tokyo). Analytical grade fenpyroximate(purity, 99.8%) and standards (**II**–**VIII**) were also supplied by Nihon Nohyaku Company (Figure 1). All solvents were HPLC grade, and other chemicals were reagent grade. Water for reagent use was obtained from a Milli-Q RO-4 purification system (Millipore, Bedford, MA).

Test System. The test system (Figure 2) consisted of autoclaved, quartz vessels (7.3 cm i.d. × 7.5 cm internal height), fitted with a sampling port for introduction of sample and with air inlet and outlet ports for maintaining air flow. Buffer, 0.01 M KH_2PO_4, pH 7, was filter-sterilized (0.2-µm filter, Nalge Co., Rochester, NY) before adding [^{14}C]fenpyroximate. Each vessel contained 200 mL of buffer to which [^{14}C]-fenpyroximate, dissolved in 0.2 mL of acetonitrile, was added to give a final concentration of 10 ppb (2.37×10^{-8} M) and approximately 200 000 dpm. Each sample was dosed, irradiated, extracted, and analyzed independently. Using a peristaltic pump, filter-sterilized air was drawn over the sample and into traps containing ethylene glycol and 1 N NaOH for the collection of volatiles. These traps were set up separately for each of the 4-h samples in phase I, and for each of the 73-h samples in phase II, for both irradiated samples and dark controls. Duplicate vessels were irradiated with constant cooling and stirring. A Suntest CPS (Heraeus DSET Laboratories, Phoenix, AZ) fitted with a 1 KW xenon lamp (radiant length, 29 cm) was used as the source of light. Filters were mounted to exclude UV radiation below 290 nm. The temperature of the irradiated samples was controlled to 25 ± 1 °C by continuously circulating chilled water.

Calibration of the Xenon Lamp. As a standard against which to compare the output of the xenon lamp, a model of the solar wavelength distribution was generated for a clear

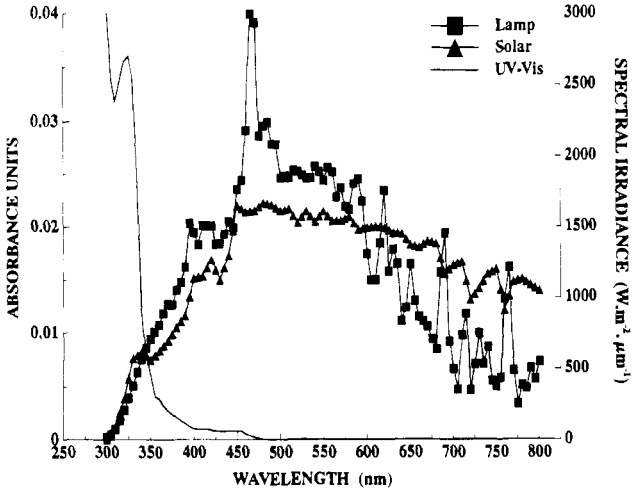

Figure 3. Comparison of the ultraviolet–visible spectrum of fenpyroximate (solid line) with the wavelength distributions of natural sunlight (triangles) and of the xenon lamp (squares).

day on June 29 in mid-northern latitudes at sea level using LOWTRAN 7 (Kneizys, 1988), solar simulation software developed by the U.S. Air Force. Lamp intensity was adjusted to 110% of the solar intensity in the 290–385-nm region of the spectrum (50.0 ± 0.1 $W \cdot m^{-2}$) using an ultraviolet (UV) radiometer (Eppley Laboratories, Inc., Newport, RI) filtered to this region of the spectrum. At this setting, the spectral distribution of the xenon lamp, at the level of the sample, approximated that of natural sunlight (Figure 3). The spectral distribution of the xenon lamp was observed using a GS4100 Intelligent Radiometer (EG&G Gamma Scientific, San Diego, CA) with transfer optics including a quartz window, a turning mirror in the beam, and a model NM-3DH spectrometer (EG&G). This system was standardized using a model HL994 lamp mounted in a model RS10A head (both from EG&G) and calibrated against NIST standards by EG&G. The integration of spectral irradiance for the xenon lamp between 290 and 800 nm yielded an exposure rate of 609 ± 3 $W \cdot m^{-2}$, a value comparable to the corresponding solar power density of 603 $W \cdot m^{-2}$ under the conditions listed above.

Sample Exposure and Processing. Duplicate samples were irradiated under the above conditions for the following intervals: 0.5, 1, 2, 3, and 4 h for phase I and 4, 12, 24, 48, and 73 h for phase II. Duplicate controls were incubated in darkness at 25 ± 1 °C for intervals of 4 h for phase I and 73 h for phase II. Duplicate 0-h samples were extracted immediately after dosing. The sterility of all samples from the 0-, 4-, and 73-h sampling intervals was verified by plating triplicate 0.1-mL aliquots onto nutrient agar and incubating for at least 2 days before visual inspection of agar plates for colony formation. After irradiation, the pH of each sample was verified (7 ± 0.2) using an Orion 301 meter (Orion Research Inc., Cambridge, MA). All samples were extracted twice with 100 mL of ethyl acetate immediately after harvesting, and the extracts were combined, reduced to 5–10 mL on a rotary evaporator, evaporated to dryness under a stream of nitrogen, and reconstituted in 1 mL of acetonitrile. Unless otherwise noted, radioactivity was monitored by analyzing aliquots in 10 mL of Aquasol II (E. I. du Pont de Nemours Co., Boston, MA) in triplicate by liquid scintillation counting (LSC) on a Beckman LS5000 or LS6000 (Beckman Instruments, Fullerton, CA). Triplicate aliquots of 1 mL from the NaOH trap were analyzed by LSC in 10 mL of Atomlight (Du Pont) and from the EG trap in Aquasol II.

High-Pressure Liquid Chromatography (HPLC). The ethyl acetate extracts were analyzed using a C-18 AQ-303 4.6 × 250 mm column (YMC, Inc., Wilmington, NC), fitted with a C-18 precolumn and maintained at 40 °C using a column heater (Model C2282, Rainin Instrument Co., Woburn, MA). Samples were mixed with equal volumes of water, and 100–200 μL was injected using a Waters (Marlborough, MA) autosampler, model Wisp 717. A Waters 600 pump and 600E

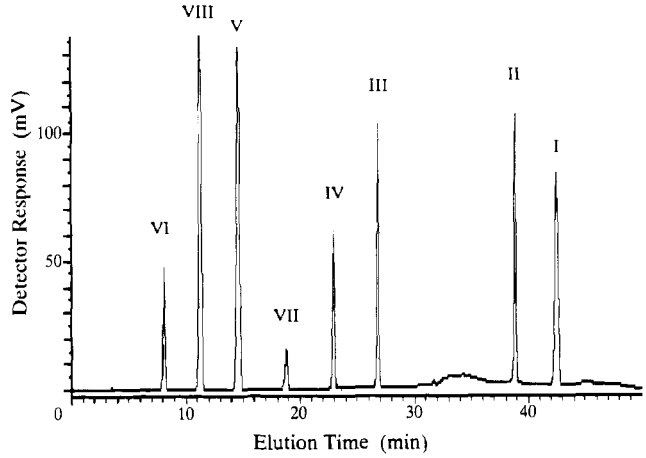

Figure 4. HPLC chromatogram of potential degradates shown in Figure 1 detected at 254 nm and separated using a C-18 column with the gradient described in the text.

controller generated the following gradient at a flow rate of 1.2 mL/min:

time	%A	%B	curve number
initial	65	35	(not applicable)
25 min	35	65	7 (concave gradient)
40 min	25	75	2 (steep convex gradient)
45 min	65	35	6 (linear gradient)
50 min	65	35	6 (linear gradient)

Standards of potential degradates were detected using a UV detector (Applied Biosystems 757, Figure 4) at 254 nm to establish retention times. Radiolabeled degradates were detected and quantitated using a Ramona 90 radiochemical detector with a 600-μL flowcell (Raytest USA Inc., Wilmington, DE) pumping Flo-Scint II scintillation fluid (Packard Instruments, Meriden, CT).

Thin-Layer Chromatography (TLC). The identities of degradates were confirmed on two samples irradiated for 4 and 24 h using the following two-dimensional TLC method: 50 μL of each sample was applied to separate 20 × 20 cm F_{254} silica plates (E. Merck, Darmstadt, Germany) 2 cm from the bottom and from the left edge of the plate. Each plate was scored 3 cm from the top of the plate in both dimensions. Nonradioactive standards (**I–VIII**) were applied to the same origin as the sample and to spots 2 cm from the lower edge of each dimension within the 3-cm-wide lane created by the scoring (Figure 5). Each plate was developed twice in the first dimension using *n*-hexane:benzene:diisopropyl ether (1:1:2, v:v) and once in the second using benzene:dioxane:acetic acid (95:25:4, v:v). Standards were located using fluorescence quenching under UV light, and radioactivity was detected using a two-dimensional scanner (Ambis, Inc., San Diego, CA).

Ultraviolet–Visible Scan. Pyrazole–[^{14}C]fenpyroximate (3×10^{-4} M in acetonitrile) was scanned from 290 to 700 nm using a dual-beam Cary 17 D spectrophotometer (Varian, Sunnyvale, CA) with a 1-cm path length cell, using acetonitrile in the reference cell. No spectrum is reported for fenpyroximate in water, due to its low solubility (14.7 ppb).

RESULTS

Mass Balance. The total recoveries of radioactivity applied (as determined from analyzing triplicate aliquots of the ethyl acetate and of the aqueous fractions from each sample) were averaged for each set of duplicate samples to give means which ranged from 91.9 to 110% in phase I and from 99.0 to 102% in phase II. The amount of applied radioactivity trapped as volatiles was less than 0.3% for phase I and less than 1% for phase II.

High-Pressure Liquid Chromatography (HPLC). The ethyl acetate extracts were analyzed by HPLC. The

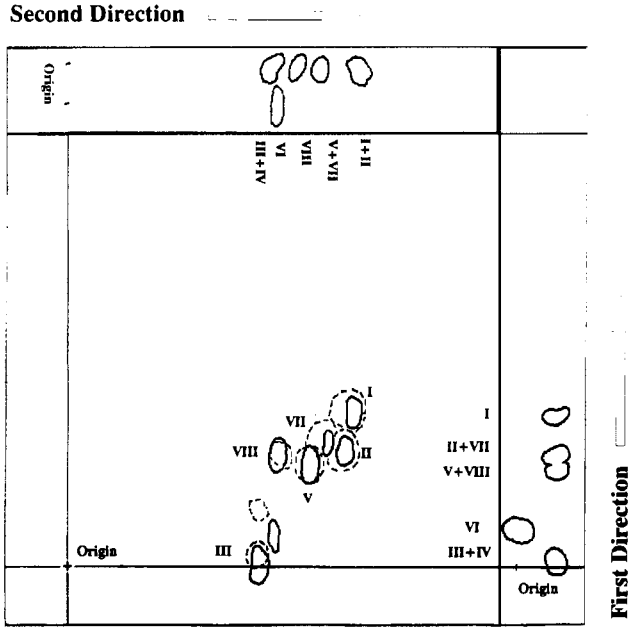

Figure 5. Two-dimensional thin layer chromatography of the ethyl acetate extract of an aqueous solution of [^{14}C]fenpyroximate irradiated under a xenon lamp for 24 h at pH 7. Radioactivity (represented by dashed lines) was located by two-dimensional radioscanner. The indicated nonlabeled standards were each chromatographed in one dimension on the margins of the plate and were also spotted on the same origin as was the radiolabeled sample. Nonlabeled standards were located by fluorescence quenching (represented by solid lines).

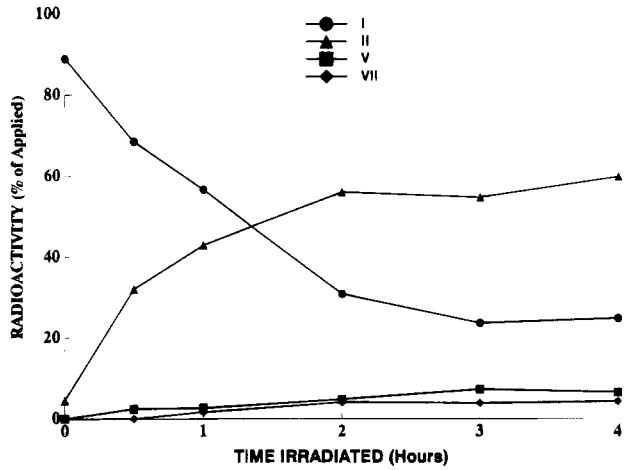

Figure 6. Phase I: kinetics of photodegradation of **I** and formation of degradates (**II, V, VII**) at pH 7 by irradiation with a xenon lamp.

distribution of radioactivity among the chromatographic peaks is shown in Figures 6 and 7. Each data point represents the mean of duplicate samples irradiated and analyzed separately and expressed as the percentage of the applied radioactivity detected in each peak. During phase I, the recovery of [^{14}C]fenpyroximate declined from 88.9% in the 0-h samples to 24.8% in the 4-h samples, while **II**, the primary degradation product, increased from 4.5 to 59.8% over the same period. In addition to **II**, small amounts of **V** (up to 7.3% at 3 h) and **VII** (up to 4.1% at 2 h) were formed. By 4 h of irradiation, the level of **II** had reached its highest value, as illustrated by the plateau in Figure 6. Therefore, 4 h was chosen as the shortest sampling time for phase II, the part of the study designed to characterize its degradation. The concentration of **I** did not change significantly between 3 and 4 h of irradiation.

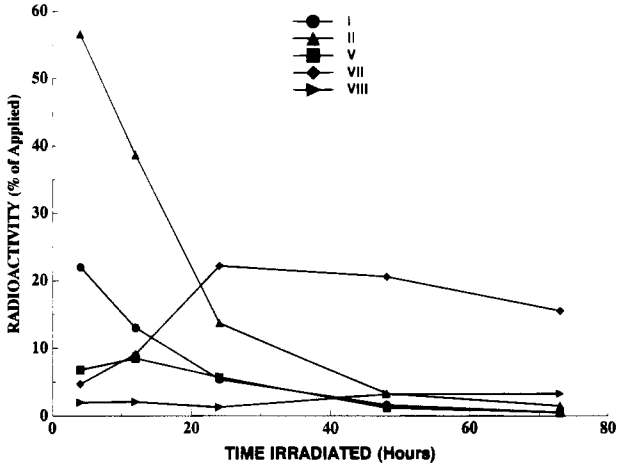

Figure 7. Phase II: kinetics of photodegradation of **I** and **II** and formation of degradates (**V, VII, VIII**) at pH 7 by irradiation with a xenon lamp.

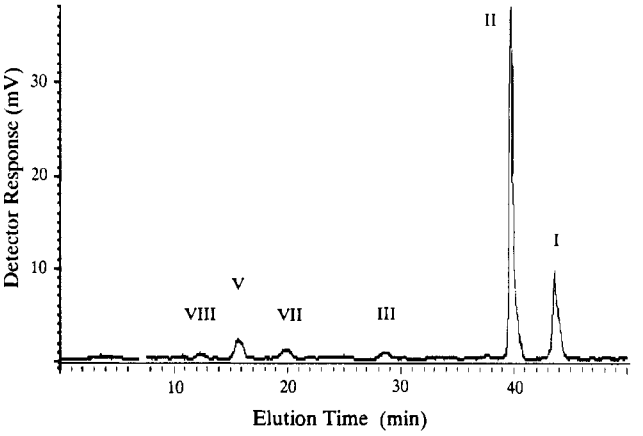

Figure 8. Radiochromatogram of the ethyl acetate extract of an aqueous solution of fenpyroximate irradiated under a xenon lamp for 4 h at pH 7.

During phase II, as the exposure interval increased from 4 to 73 h, the level of **II** decreased from 56.6% to 1.5% (Figure 7). The level of **VII** increased to its maximum, 22.2% at 24 h, after which it gradually declined to 15.5% at 73 h. The level of fenpyroximate continued to decrease and, at 73 h, it accounted for only 0.5% of the applied radioactivity. The level of **V** increased to a maximum of 8.5% with 12 h of exposure. Minor peaks of **III** and **VIII** were also seen, each representing less than 10% of applied radioactivity at any sampling time. A typical chromatogram for an irradiated sample is shown in Figure 8 and a set of analytical standards in Figure 4.

Rate Constants and Quantum Yield. On the basis of phase I data for fenpyroximate shown in Figure 6, the first-order rate constant was calculated as follows: the natural logarithm of the percentage of compound remaining at each exposure interval was plotted against that interval, and the linear regression was calculated for the plot. The last point (representing the 4-h interval) was omitted from this regression, since it did not lie on the approximately straight line defined by the remaining points, and therefore did not correspond to first-order kinetics (Figure 9). The negative slope (0.46) of this regression line represents the first-order rate constant, k. Likewise, on the basis of phase II data shown in Figure 7, k was calculated (0.066) for **II**, omitting the last data point at 73 h (Figure 10). The half-lives ($t_{1/2}$) were calculated according to the relationship: $t_{1/2} = (\ln 2)/k$, which gave the result of 1.5 h

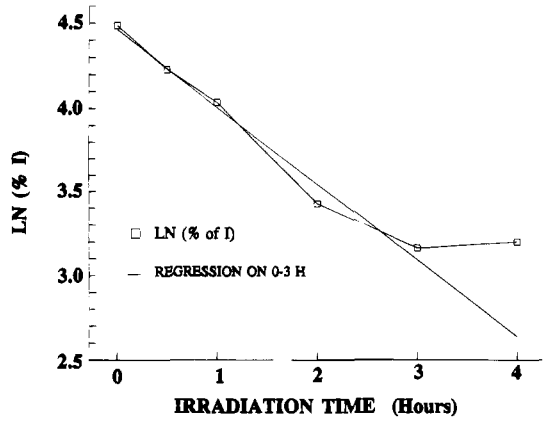

Figure 9. Phase I: logarithm of fenpyroximate (expressed as a percentage of the applied radioactivity) plotted against irradiation time. The regression line (whose negative slope represents the first-order rate constant for **I**) was calculated without the 4-h data point.

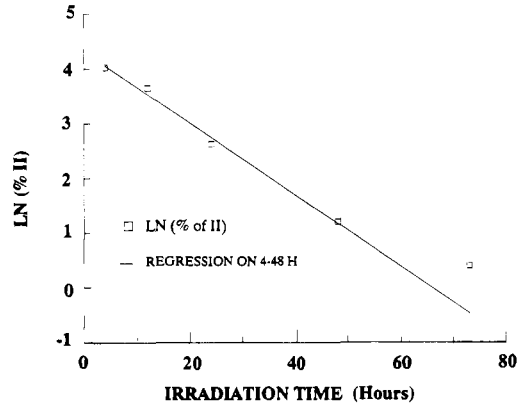

Figure 10. Phase II: logarithm of **II** (expressed as a percentage of the applied radioactivity) plotted against irradiation time. The regression line (whose negative slope represents the first-order rate constant for **II**) was calculated without the 73-h data point.

for fenpyroximate and 10.5 h for its geometric isomer (**II**). From the rate constant for fenpyroximate degradation, using eq 1, a quantum yield of 7.5% was calculated.

Thin-Layer Chromatography (TLC). Two-dimensional TLC was used to qualitatively confirm the identities of the degradates for two phase II samples, one irradiated for 4 h and the other for 24 h. Figure 5 shows the results for the 4-h sample with solid lines representing the fluorescence quenching of the cochromatographed nonlabeled qualitative standards and the broken lines representing [^{14}C]labeled compounds, fenpyroximate and its degradates. Similar data were obtained for the sample irradiated for 24 h (not shown). These TLC plates confirmed the presence of **I, II, III, V, VII,** and **VIII**. Compounds **III** and **IV** were not well enough resolved to distinguish between the two by TLC alone. However, since they were well-separated by HPLC (Figure 4), and since **III** but not **IV** was detected by HPLC, the spot observed on TLC confirms **III**.

Dark Controls. The control samples, incubated in the dark for either 4 or 73 h, did not change significantly over the incubation period. This indicates that fenpyroximate is stable to hydrolysis within the conditions and time frame of this study and that the degradation observed in this study can be attributed to photolysis only.

Ultraviolet–Visible Spectrum. The UV–visible spectrum of 3×10^{-4} M fenpyroximate shows a peak at about 325 nm. Figure 3 illustrates the wavelength interval over which the absorption by fenpyroximate overlaps emission by the optically filtered xenon lamp.

Table 1. Data Used To Calculate Wavelength-Averaged Quantum Yield for Fenpyroximate

wavelength λ, nm	absorbance A(λ) (base 10)	molar absorptivity $\alpha(\lambda)$ (base e), cm^2/mol	spectral irradiance I(λ) W·m^{-2}·μm^{-1}	$\lambda \times \alpha(\lambda) \times$ I(λ) $\times$ 1.505×10^{-11}
300	0.041	317508	7.28	0.010
305	0.035	271044	96.55	0.120
310	0.032	247811	185.81	0.215
315	0.034	263299	316.07	0.395
320	0.035	271044	446.32	0.583
325	0.036	278788	612.88	0.836
330	0.035	271044	779.44	1.049
335	0.024	185858	801.13	0.751
340	0.012	92929	822.82	0.391
345	0.008	61953	741.50	0.239
350	0.006	46465	660.17	0.162
355	0.004	30976	749.21	0.124
360	0.004	30976	838.25	0.141
365	0.003	23232	854.48	0.109
370	0.003	23232	870.71	0.113
375	0.002	15488	909.06	0.079
380	0.002	15488	947.42	0.084
385	0.002	15488	1006.58	0.090
390	0.002	15488	1065.75	0.097
395	0.001	7744	1207.67	0.056
400	0.001	7744	1349.59	0.063
405	0.001	7744	1349.99	0.064
410	0.001	7744	1350.38	0.065
415	0.001	7744	1406.19	0.068
420	0.001	7744	1461.99	0.072
425	0.001	7744	1370.06	0.068
430	0.001	7744	1278.12	0.064
435	<0.001	N/C	1372.43	N/C
440	<0.001	N/C	1466.74	N/C

$\Sigma[\lambda \times \alpha(\lambda) \times I(\lambda) \times 1.505 \times 10^{-11}] = 6.105\ h^{-1}$

$k = 0.46\ h^{-1}$; quantum yield = $k/6.105 = 7.5\%$

[a] The absorbance data is derived from the ultraviolet–visible spectrum of 3×10^{-4} M fenpyroximate. The irradiance values for the xenon lamp (based on a band with ± 2.5 nm about each indicated wavelength) were measured using a radiometer. N/C = not calculated.

DISCUSSION

Calculation of Quantum Yield. Equation 1 was used to calculate Φ, the quantum yield.

$$\Phi = \frac{k}{\sum_{\lambda = 300\ \text{by}\ \Delta\lambda}^{430} \alpha(\lambda) \times \lambda \times I(\lambda) \times (1.505 \times 10^{-11})} \quad (1)$$

where Φ is the quantum yield (dimensionless), k is the first-order rate constant [calculated as the negative slope of the regression line where ln(% of compound remaining) is plotted against time] (h^{-1}), λ is wavelength (nm), $\Delta\lambda$ is the wavelength interval (nm) ($\Delta\lambda = 5$ nm), I(λ) is spectral irradiance (in W·m^{-2}·μm^{-1}), and $\alpha(\lambda)$ is molar absorptivity (in cm^2·mol^{-1}) and $\alpha(\lambda) = 2.3\ A(\lambda)/Cl$, where $A(\lambda)$ is absorbance (dimensionless) determined in separate experiment at each wavelength interval, C is the concentration (M) at which the absorbances were determined, and l is the path length (in cm). The summation begins at 300 nm because light intensity below that wavelength is virtually zero (Figure 3). The summation ends at 430 nm because the absorbance of fenpyroximate above that wavelength is zero, and would therefore contribute nothing to the sum. Table 1 shows the data applied to this formula. This formula was

derived (see the supplementary material) such that the experimental values could be used directly, as obtained from the ultraviolet–visible spectrophotometer (absorbance at each wavelength in determination of absorptivity, $\alpha(\lambda)$) and from the spectral radiometer (spectral irradiance at each wavelength, $I(\lambda)$) used to calibrate the xenon lamp. The formula is similar to others provided in the environmental fate literature (e.g., Weerasinghe et al., 1992) in that it represents a wavelength-averaged quantum yield. The constant (1.505×10^{-11}) takes into consideration the conversion of spectral irradiance from watts to einsteins. The determination of $\alpha(\lambda)$ should ideally be performed on an aqueous solution of the experimental compound. However, for compounds (such as fenpyroximate) whose slight solubility in water precludes such measurement, the use of a polar organic solvent, such as acetonitrile, whose refractive index approaches that of water, is recommended (Zepp, 1978).

Degradation Kinetics. The primary feature of fenpyroximate degradation is its biphasic nature: For the first 3 h of irradiation, the degradation of fenpyroximate approximated first-order kinetics (Figure 9), remaining at approximately the same concentration throughout the fourth hour of irradiation before again decreasing in concentration (Figure 10). Since the primary product of degradation was the geometric isomer (**II**), it is possible that, as the concentration of **II** built up (due to its longer half-life relative to that of **I**) the reverse reaction (conversion to **I**) may have transiently achieved approximately the same rate as the forward reaction. On a larger time scale, as other photoproducts (primarily **V** and **VII**) formed irreversibly, both **I** and **II** decreased to levels near zero. Because results at the fourth hour did not follow first-order kinetics, they were excluded from the calculation of the rate constant, k. Likewise, the final point (at 73 h) of phase II was eliminated from the calculation of the second rate constant, since it does not follow first-order kinetics (Figure 10), probably due to the uncertainties of measuring small quantities of radioactivity. Rapid photodegradation of fenpyroximate is consistent with the significant extent to which its absorption spectrum overlaps the emission spectrum of the xenon lamp (Figure 3).

CONCLUSIONS

The quantum yield indicates that, of the photons absorbed by fenpyroximate, 7.5% cause degradation. By comparison, most photolabile pesticides have quantum yields of less than 1% (Draper and Wakeham, 1993), indicating that fenpyroximate converts photon energy to chemical reaction at a significantly higher than usual efficiency. As calculated, the quantum yield represents an average over the wavelengths at which light is absorbed; it may vary within narrower bands of this spectrum. The rapid degradation of fenpyroximate and of its geometric isomer show that, when exposed to sunlight, they would not accumulate in an aqueous environment.

ACKNOWLEDGMENT

We gratefully acknowledge financial support for this project from Nihon Nohyaku, Ltd. Also, we sincerely appreciate the expertise of Dr. Russell H. Barnes, Jr., who verified the calculations.

Supplementary Material Available: Derivation of the formula used to calculate quantum yield directly from experimental values (4 pages). Ordering information is given on any current masthead page.

LITERATURE CITED

Bard, L. New instrumental approach for evaluating photodegradation of chemicals. Technical Report; DSET Laboratories, Phoenix, AZ, 1989.

Dauben, W.; Kellogg, M. Wavelength dependency in the photochemistry of 1,3-cyclohexadienes. *cis*-bicyclo[4.3.0]-nona-2,4-diene to *cis,cis,trans*-1,3,5-cyclononatriene valence tautomerism. *J. Am. Chem. Soc.* **1971**, *93*, 3805–3807.

de Mayo, P.; Shizuka, H. On the mechanism of photocycloaddition of thiobenzophenone at 366 nm. *J. Am. Chem. Soc.* **1973**, *95*, 3942–3947.

Draper, W.; Wakeham, D. Rate constants for metam-sodium cleavage and photodecomposition in water. *J. Agric. Food Chem.* **1993**, *41*, 1129–1133.

Larson, R.; Schlauch, M.; Marley, K. Ferric ion promoted photodecomposition of triazines. *J. Agric. Food Chem.* **1991**, *39*, 2057–2062.

Leifer, A. *The Kinetics of Environmental Aquatic Photochemistry, Theory and Practice*; ACS Professional Reference Book; American Chemical Society: Washington, DC, 1988.

Nishizawa, H.; Hirano, A.; Hasegawa, T.; Suzuki, T.; Uchida, M. *Photodegradation of fenpyroximate in water*; Report Number ILSR-E-90-057A; Nihon Nohyaku Company, Ltd.: Tokyo, 1990.

Sugihara, Y.; Wakabayashi, S.; Murata, I.; Jinguji, M.; Nakazawa, T.; Persy, G.; Wirz, J. Upper excited state reactivity and fluorescence of fuse 8-cyanoheptafulvenes. *J. Am. Chem. Soc.* **1985**, *107*, 5894–5897.

Test Guideline: Phototransformation of Chemicals in Water. Part A: Direct Phototransformation; Richtlinien für die Prüfung von Pfanzenschutzmitteln im Zulassungsverfahren, Teil IV, 6–1; Biologische Bundesanstalt für Land- und Forstwirtschaft, Bundesrepublik Deutschland; Umweltbundesamt: Berlin, 1990.

Testa, R.; Dolfini, E.; Reschiottor C.; Secchi, C.; Biondi, P. GLC determination of nifedipine, a light sensitive drug, in plasma. *Il Farmaco Ed. Prat.* **1979**, *34*, 463–473.

Thoma, K.; Kerker, R. Presented at the Association of Pharmaceutical Producers Symposium, Regensburg, Germany, April 1992.

Thoma, K.; Klimek, R. Studies on photoinstability of nifedipine. Part 1: Kinetics of degradation and reaction mechanism. *Pharm. Ind.* **1985**, *47*, 207–215.

U.S. Environmental Protection Agency. *Pesticide Assessment Guidelines, Subdivision N, Section 161-2. Chemistry: Environmental Fate;* Office of Pesticide and Toxic Substances: Washington, D.C., 1982.

Weerasinghe, C.; Mathews, J.; Wright, R.; Wang, R. Aquatic photodegradation of albendazole and its major metabolites. 2. Reaction quantum yield, photolysis rate, and half-life in the environment. *J. Agric. Food Chem.* **1992**, *40*, 1419–1421.

Woodburn, K; Batzer, F.; White, F.; Schultz, M. The aqueous photolysis of triclopyr. *Environ. Toxicol. Chem.* **1993**, *12*, 43–55.

Zepp, R. Quantum yields for reaction of pollutants in dilute aqueous solution. *Environ. Sci. Technol.* **1978**, *12*, 327–329.

Zepp, R.; Cline, D. Rates of direct photolysis in aquatic environment. *Environ. Sci. Technol.* **1977**, *11*, 359–366.

Received for review July 6, 1994. Revised manuscript received November 3, 1994. Accepted November 22, 1994.[⊗]

JF940361W

[⊗] Abstract published in *Advance ACS Abstracts,* January 1, 1995.